The Fourth Italian Workshop on Landslides

An exponential matrix method for the buckling analysis of underground pipelines subjected to landslide loads

Eugenio Ruocco[a,*], Raffaele Di Laora[b], Vincenzo Minutolo[a]

[a]Second University of Naples, Department of Civil Engineering, Design, Building and Environment, Via Roma 29, Aversa 81031,Italy
[b]University of Ferrara, Department of Ingegneria, Via Saragat 1, Ferrara 44122, Italy

Abstract

Due to their dimensions, long pipelines often cross areas that are highly susceptible to landslides. In Italy, this problem requires special attention, as many slow-moving landslides interact with buried pipelines. The paper analyzes such interaction problem with particular reference to buckling analysis, tackling the solution of the governing equations by an exponential matrix method. In the paper the basic equation, its computational aspects and numerical analysis options are outlined. Representative results of the proposed methodology and potential applications on buckling analysis of buried pipes are presented.

© 2016 The Authors. Published by Elsevier B.V. This is an open access article under the CC BY-NC-ND license (http://creativecommons.org/licenses/by-nc-nd/4.0/).
Peer-review under responsibility of the organizing committee of IWL 2015

Keywords: Buckling; buried pipelines; landslides.

1. Introduction

In recent years the use of pipelines for the transportation of oil and gas has greatly increased in many parts of the world. Long pipelines often cross areas susceptible to slow-moving landslides[1] and it is therefore important to ensure their integrity under the stress deriving by the compressive load induced by the ground motion. In some circumstances buckling phenomena can also occur[2]. As critical load is in inverse proportion to the square root of the pipe length embedded in the moving ground, long pipes can buckle under very low values of the compressive load, and can be cause of human loss as well as economic and environmental damage. For example, the Guanabara oil spill, which occurred in Brazil on January 2000 and caused the spread of 1.3 million liters of oil into Guanabara bay, was caused by lateral buckling of offshore pipeline that eventuated in local buckling and rupture of the pipe wall[3].

* Corresponding author. Tel.: +0-000-000-0000 ; fax: +0-000-000-0000 .
  E-mail address: author@institute.xxx

Nomenclature

E	modulus of elasticity
I	Second moment of cross-sectional area
L	Overall length of pipeline
L_0	Imperfection half-wavelength
P_i	Concentrate load (anchorages)
R_e	External radius of circular pipe
R_i	Internal radius of circular pipe
q	Distributed load (landslides)
k_s	Winkler springs (elastic foundation)
u	Generalized in-plane displacement in buckling mode
w	Generalized out-of-plane displacement in buckling mode
θ	Bending rotation

Similarly, buckling of onshore inclined pipelines was observed during construction in Colombia in the last years of the twentieth century[4].

Consequently, effective constant monitoring[5] and prediction of buckling load and effective measures against this phenomenon are important aspects of design of pipelines[6,7]. However, buckling of pipes is quite complicate, involving complex pipe-soil interaction, dependence of initial imperfections and effect deriving from second-order displacement field.

The scientific interest on the different aspects of the buckling analysis of buried pipes is proved by the growing number of papers devoted to this topic. For instance, Zhang *et al.*[8] proposed a finite element model for analyzing the buckling behavior of a buried pipeline impacted by a cube-shaped rockfall, analyzing the effects of the impact velocity, buried depth, impact position, and base area on the stress of the pipeline. Xue *et al*[9]. presented a first order shear theory for the buckling analysis of cylindrical sandwich pipes subjected to undersea water pressure. In their model the authors examine the change of the circumferential radius due to the radial deflection of the cylindrical sandwich shell and its effect on the bending moments.

This paper presents a simplified numerical model that captures the main features of the buckling of a beam on an elastic foundation. The effects of various parameters such as the amplitude of initial imperfection and presence of anchorage points are investigated. In the ensuing, the numerical model is derived in detail and some representative results are discussed.

2. Method

The problem under investigation consists of a circular pipeline of length L and mean radius R depicted, with the local coordinate system adopted in the paper, in Fig. 1. Let the pipeline be subjected to a lateral external pressure q and concentrated loads P applied in different points of the pipe, both acting in the axial direction, and characterized by a continuous elastic restraints of stiffness k_s. Also, in order to simulate the presence of local geometric imperfection, a variable cross-sectional moment of inertia $I(z)$ has been considered.

The main assumptions are that a) the plane section remains plane and normal to the axis of the beam before bending and b) the axis of the beam is inextensible. Such hypotheses are satisfied by the following choice of the displacement field:

$$s_x\left(x,z\right)=w\left(x\right), \ s_z\left(x,z\right)=u\left(z\right)+x\theta\left(z\right), \ \theta\left(z\right)=-\frac{dw\left(z\right)}{dz} \tag{1}$$

In order to capture the non-linear behavior ruling the buckling of the beam, one can consider the strain tensor:

$$\varepsilon_z = \frac{du}{dz} + z\frac{d\theta}{dz} + \frac{1}{2}\left(\frac{dw}{dz}\right)^2 \tag{2}$$

in which, according with the von Karman hypothesis[10,11], the second-order terms deriving from the in-plane displacement s_z have been considered negligible.
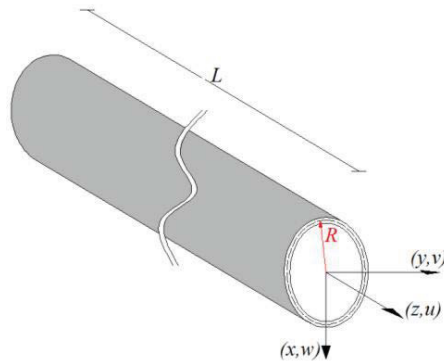

Fig. 1. Geometry and reference system adopted for the beam.

The governing equations for the buckling of Euler beam with continuous elastic restraints represented in Fig. 2 is given by:

$$\frac{d^2}{dz^2}\left(EI(z)\frac{d^2w}{dz^2}\right) + P_i\frac{d^2w}{dz^2} + \frac{d}{dz}\left(\int_0^z q(z)dz\frac{dw}{dz}\right) + k_s w = 0 \tag{3}$$

where $q = q_z$ is the distributed load and P_i the concentrated force applied in the ith point acting in the axial direction.

The boundary conditions involve specifying one element of each of the following two pairs at *x=0* and *x=L*:

$$\frac{dw}{dz} = 0 \quad or \quad \frac{d^2w}{dz^2} = 0$$
$$w = 0 \quad or \quad EI\frac{d^3w}{dz^3} - N\frac{dw}{dz} = 0 \tag{4}$$

Since Eq. (3) cannot be solved in closed form, a numerical approach has to be adopted. In this paper the exponential matrix method, previously employed for solving differential equations in one[12] and two[13] dimensions, is here proposed for solving the eigenproblem related to the critical behaviour of Euler beams.
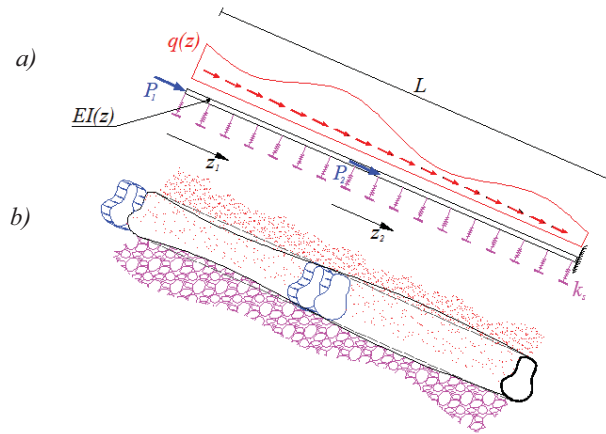
Fig. 2. *a*) mathematical and *b*) physical model of the pipe.

The original version of this method approximates the out-of-plane displacement *w* with a sum of N_1 decaying exponential functions:

$$w(z) \cong w_{N_1} = \sum_{n_1=0}^{N_1} a_{n_1} e^{-n_1 z} \tag{5}$$

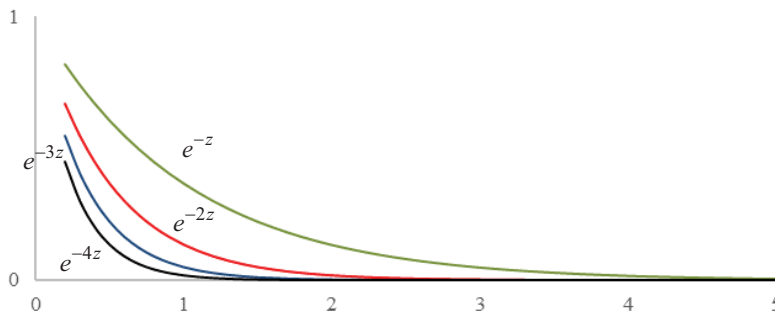the first four of which are represented in Fig.3, multiplied by the unknown coefficients a_{N_1}.

Fig.3. Exponential functions adopted for the approximate solution.

The method exploits the properties of the exponential function for obtaining a simple but powerful method for solving general differential equations. However, the decaying nature of the exponential basis results to be highly unstable for solving the eigenvalue problems ruling the buckling problem. For such a reason the original method has been here enriched with two more families of trigonometric function, i.e.:

$$w(z) \cong w_{N_1} + w_{N_2} + w_{N_3} = \sum_{n_1=0}^{N_1} a_{n_1}^{[1]} e^{-n_1 z} + \sum_{n_2=0}^{N_2} a_{n_2}^{[2]} \sin n_2 z + \sum_{n_3=0}^{N_3} a_{n_3}^{[3]} \sin n_3 z \tag{6}$$

the first four of which are represented in Fig. 4. The exponential method with the new basis maintains the same advantages of the original method returning, in the same time, a more reliable numerical procedure.

By adopting the displacement field (6), it is possible to rewrite the integrodifferential equation (3) in the following algebraic form:

$$\mathbf{C}_1(z) \cdot \mathbf{a}_1^T + \mathbf{C}_2(z) \cdot \mathbf{a}_2^T + \mathbf{C}_3(z) \cdot \mathbf{a}_3^T = 0 \tag{7}$$

$\cos 4z$
$\cos z$
$\cos 3z$
$\cos 2z$

$\sin 4z$
$\sin 3z$
$\sin 2z$
$\sin z$

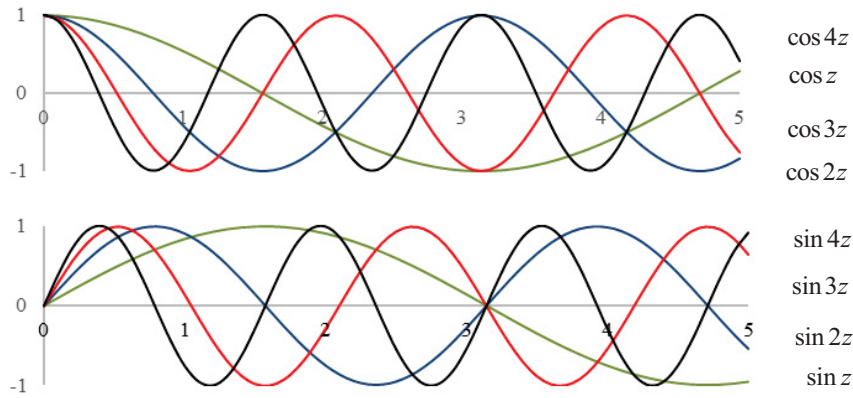Fig. 4. Trigonometric functions adopted for the approximate solution.

in terms of the known coefficients:

$$\mathbf{C}_1(z) = \mathbf{E}_1(z) \cdot \left(\mathbf{M}_1^4 + \left(\frac{P}{EI(z)} + \frac{\int_0^z q dz}{EI(z)} \right) \cdot \mathbf{M}_1^2 + q(z) \cdot \mathbf{M}_1^1 + \frac{k_s}{EI(z)} \cdot \mathbf{I}_1 \right)$$

$$\mathbf{C}_2(z) = \mathbf{E}_2(z) \cdot \left(i \cdot \mathbf{M}_2^4 + \left(\frac{P}{EI(z)} + \frac{\int_0^z q dz}{EI(z)} \right) \cdot i \cdot \mathbf{M}_2^2 + q(z) \cdot \mathbf{M}_2^1 + \frac{k_s}{EI(z)} \cdot i \cdot \mathbf{I}_2 \right) \tag{8}$$

$$\mathbf{C}_3(z) = \mathbf{E}_3(z) \cdot \left(\mathbf{M}_3^4 + \left(\frac{P}{EI(z)} + \frac{\int_0^z q dz}{EI(z)} \right) \cdot \mathbf{M}_3^2 + q(z) \cdot i \cdot \mathbf{M}_3^1 + \frac{k_s}{EI(z)} \cdot \mathbf{I}_3 \right)$$

depending on the applied loads, the beam properties and the spring stiffnesses, and of the unknown terms collected in the vectors:

$$\mathbf{a}_1 = \left[a_1^{[1]} \; a_2^{[1]} \; ... \; a_{N_1}^{[1]} \right]$$

$$\mathbf{a}_2 = \left[a_1^{[2]} \; a_2^{[2]} \; ... \; a_{N_2}^{[2]} \right] \tag{9}$$

$$\mathbf{a}_3 = \left[a_1^{[3]} \; a_2^{[3]} \; ... \; a_{N_3}^{[3]} \right]$$

In Eq. (8) i is the imaginary unit, the matrices $\mathbf{E}_i$ collect both the exponential and trigonometric basis:

$$\mathbf{E}_1 = \frac{1}{2} \left[\mathbf{e}^{-n_1 \cdot z} \quad \mathbf{e}^{-n_1 \cdot z} \right]; \quad \mathbf{E}_2 = \frac{1}{2} i^{k+1} \cdot \left[\mathbf{e}^{-n_2 \cdot i \cdot z} \quad \mathbf{e}^{n_2 \cdot i z} \right]; \mathbf{E}_3 = \frac{1}{2} i^k \cdot \left[\mathbf{e}^{-n_3 \cdot i z} \quad \mathbf{e}^{n_3 \cdot i z} \right] \tag{10}$$

and:

$$\mathbf{M}_1 = \begin{bmatrix} \mathbf{m}_1^k \\ \mathbf{m}_1^k \end{bmatrix}; \ \mathbf{M}_2 = \begin{bmatrix} \mathbf{m}_2^k \\ -(-\mathbf{m}_2)^k \end{bmatrix}; \ \mathbf{M}_3 = \begin{bmatrix} \mathbf{m}_3^k \\ (-\mathbf{m}_3)^k \end{bmatrix}; \ \mathbf{m}_i^k = \begin{bmatrix} 0 & 0 & & & \\ 0 & -1^k & & & \\ 0 & 0 & -2^k & & \\ 0 & 0 & 0 & \ddots & \vdots \\ 0 & 0 & 0 & \cdots & -N_i^k \end{bmatrix} \tag{11}$$

By subdividing the beam in *N* subelements and by collocating the eq. (7) in the corresponding *N+1* points (Fig. 5), it is possible to obtain the square system:

$$\begin{bmatrix} \mathbf{C}_1(x_0) & \mathbf{C}_2(x_0) & \mathbf{C}_3(x_0) \\ \mathbf{C}_1(x_1) & \mathbf{C}_2(x_1) & \mathbf{C}_3(x_1) \\ \vdots & & \\ \mathbf{C}_1(x_N) & \mathbf{C}_2(x_N) & \mathbf{C}_3(x_N) \end{bmatrix} \cdot \begin{bmatrix} \mathbf{a}_1^T \\ \mathbf{a}_2^T \\ \mathbf{a}_3^T \end{bmatrix} = \mathbf{0} \tag{12}$$

in terms of the applied loads P_i and $q(z)$. By posing $\det\big(\mathbf{C}(q(z),P_i)\big)=0$, it is finally possible to obtain the critical values of such loads.
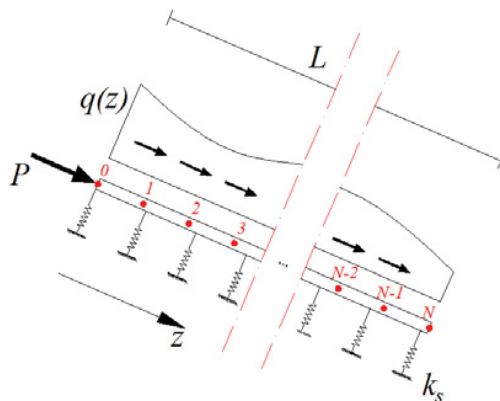

Fig. 5. Collocating points.

3. Results and discussion

The effects of various parameters on the buckling response of a pipe subjected to a landslide-generated axial load are evaluated and summarized in this section. The study considers local geometric imperfection, presence of concentrate axial load and effects of the elastic foundation. The geometric and material properties of the considered pipe, representative of typical cases encountered in real life[14], are listed in Table 1.

Table 1. Pipe properties.

Pipe external radius	R_e	11.4	cm
Pipe internal radius	R_i	10.0	cm
Second moment of cross-sectional area	I	5411	cm^4
Modulus of Elasticity	E	207	GPa

3.1. Local geometric imperfection

In this study, an imperfection δ varying along the pipe has been considered, according to the function:

$$\delta(z) = \delta_0 \sin \frac{n\pi z}{L_0} \tag{13}$$

which corresponds to a constriction of the pipe in one or more points (Fig. 6). The two main parameters describing the local geometric imperfection are the imperfection amplitude δ_0 and the half-wavelength L_0 / n.
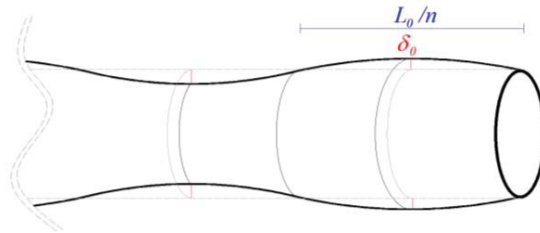

Fig. 6. Sinusoidal defect of the pipe.

As a consequence of such imperfection, both the external and the internal radii R_e, R_i and the corresponding cross-sectional moment of inertia I of the pipe change as follow:

$$R(z) = R + \delta_0 \sin \frac{n\pi z}{L_0}$$

$$I(z) = \frac{\pi}{4} \left(\left(R_e + \delta_0 \sin \frac{n\pi z}{L_0} \right)^4 - \left(R_i + \delta_0 \sin \frac{n\pi z}{L_0} \right)^4 \right) \tag{14}$$
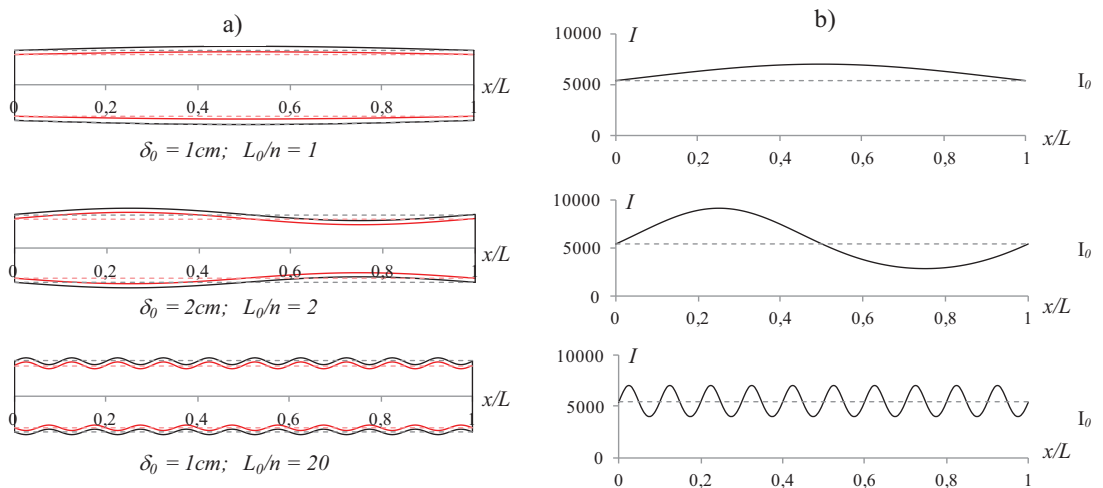

Fig. 7. *a)* Imperfect pipes and *b)* corresponding inertia.

Fig. 7 reports examples of imperfect pipes with different values of δ_0 and L_0 / n, and the corresponding variation of I. Such a figure shows that cross-sectional moment of inertia follows the same trend as the deflected shape, that is sinusoidal with a number of halfwaves equal to L_0 / n with values oscillating around I_0 corresponding to the perfect pipe. The extremes I_{max} / I_{min} depend exclusively on the ratio between δ_0 and (R_e, R_i): the larger is this ratio, the larger are differences between I_{max} / I_{min} and I_0. Table 2 reports the effect of some representative values of δ_0 on the inertia of a pipe characterized by the dimensions reported in Table 1.

Table 2. maximum/minimum second moment of cross-sectional area for different δ_0.

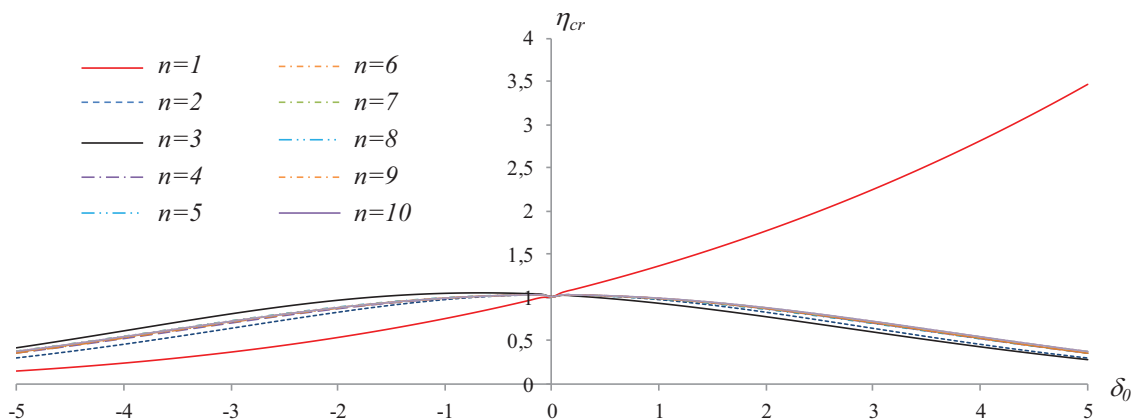| δ_0	I_{max} / I_0	I_{min} / I_0
0.1 *cm*	1.02822	0.97230
0.5 *cm*	1.14641	0.86663
1 *cm*	1.30648	0.74570
2 *cm*	1.67002	0.53870
5 *cm*	3.15178	0.15279

Fig. 8. Nondimensional critical vs. amplitude and half-wavelength of the defect.

Figure 8 reports values of $\eta_{cr} = P_{cr} / P_0$, i.e. the buckling load normalized by the critical load P_0, with reference to a pipe without imperfection, for different values of δ_0 and n. The above Figure indicates that the critical load decreases by increasing the imperfection amplitude δ_0, with values lower than $0.2P_0$ for $\delta_0 > 0.4$ cm. Moreover, it can be noticed a substantial insensibility of η_{cr} on the number of half waves n, the differences in terms of critical load being lower than 5%.

In addition to this, the results do not depend on the sign of δ_0 with the only exception of the case $n=1$, where the critical load η_{cr} increases with δ_0, assuming values greater than unity (that is, the *imperfect* pipe has a critical load greater than the perfect one) for positive values of δ_0. Such peculiarity, which may appear as counterintuitive at first sight, can be explained by observing the first imperfect pipe reported in Fig. 7, for which $n=1$. In such a case $\delta_0 > 0$ leads to a larger value of cross-sectional moment of inertia (the opposite is true for $\delta_0 < 0$).

3.2. Effect of the elastic restrains on the critical load of underground pipelines

The critical behavior of a pipeline generate by a landslide can be reduced by the stabilizing effect of the surrounding field. Such an effect can be adequately modelled by elastic restrains with a stiffeness k_s derived by the physical characteristic of the land. The next example shows the beneficial effect deriving by the presence of elastic

restrains on the critical load of a pipeline for different values of load ratio P/q, stiffness k_s and boundary conditions. In the figure symbols C, S and F identify the Clamped ($w = \varphi = 0$), Simply-supported ($w = 0$, $\varphi \neq 0$) and Free ($w \neq 0$, $\varphi \neq 0$) boundary conditions applied to the ends, so that *C-S* denotes a pipe clamped at $x = 0$ and simply supported at $x = L$, *C-F* indicates a beam clamped at $x = 0$ and free at $x = L$ and so on.

The simultaneous presence of distributed and tip forces returns the buckling capacities curves represented, for different boundary conditions, in Fig. 9: when the values of (P, q) are found under the curves, the pipe will not buckle.

Conclusions

A novel model able to determine the critical load of pipelines subjected to landslide load has been presented. The model allows for considering concentrate loads acting on a pipe of variable inertia resting on elastic foundation. Some examples have shown the potentiality of the method, as well as the effects of crucial parameters on the critical behavior of the pipeline. The model can be seen as a first step towards more complex models which can take into account, for instance, a non-linear constitutive behaviour of both pipeline and soil.
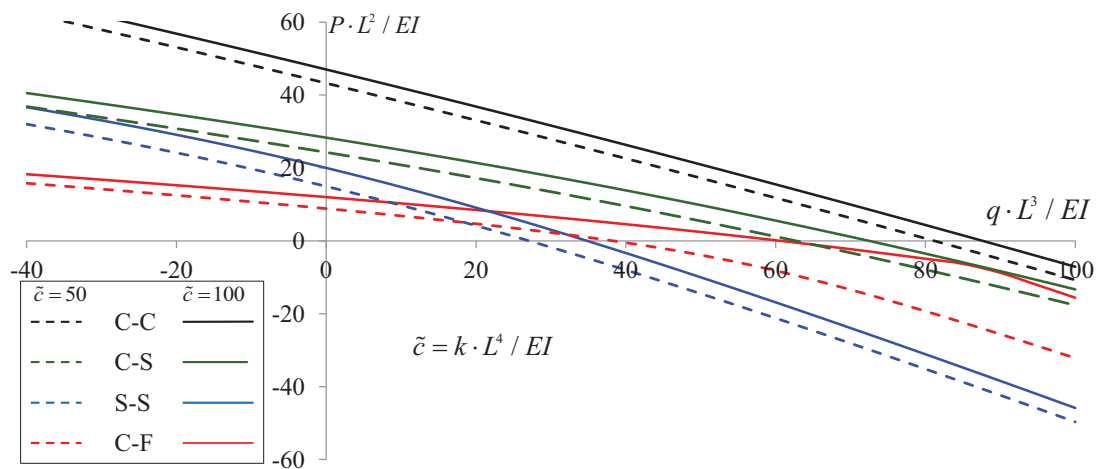

Fig. 9. Resistance domain for different *P/q* ratio and values of the elastic restrains.

References

1. Mandolini A, Minutolo V, Ruocco E. Coupling of underground pipelines and slowly moving landslides by BEM analysis. *CMES* 2001;**2**(2):39-47.
2. Zhu J, Attard MM, Kellermann DC. In-plane nonlinear localised lateral buckling of straight pipelines. *Eng Struct* 2015;**103**:37-52.
3. Costa AMD, Cardoso CDO, Amaral CDS, Andueza A. *Soil-structure interaction of heated pipeline buried in soft clay.* In: ASME conference proceedings, vol. 2002, no 36207; 2002. p.457-66.
4. Palmer AC, Tebboth L, Miles D, Calladine CR. Insability of pipelines on slopes. *J App Mech* 1999; **66**(3):794-9.
5. Bernini R, Minardo A, Ciaramella S, Minutolo V, Zeni L. Distributed strain measurement along a concrete beam via stimulated brillouin scattering in optical fibres. *Int J Geophysics* 2011; **2011**: 1-5.
6. Bransby MF, Newson TA, Brunning P. The upheaval capacity of pipelins in jetted clay blackfill. *Int J offshore Polar Eng* 2002;**12**(4):280-7.
7. Cheuk CY, Take WA, Bolton MD, Oliveira JRMS. Soil restraint on buckling oil and gas pipelines buried in lumpy clay fill. *Eng Struct* 2007;**29**:973-82.
8. Zhang J, Liang Z, Han C, Zhang H. Buckling behaviour analysis of a buried steel pipeline in rock stratum impacted by a rockfall. *Eng Fail Anal* 2015;**58**:281-94.
9. Xue J, Wanf Y, Yuan D. A shear deformation theory for bending and buckling of undersea sandwich pipes. *Comp Struct* 2015;**132**:633-43.

10. Ruocco E, Mallardo V. Buckling analysis of Levy-type orthotropic stiffened plate and shell based on different strain-displacement models. *Int J Non-linear Mech* 2013;**50**:40-47.
11. Ruocco E, Minutolo V, Ciaramella S. A generalized analytical approach for the buckling analysis of thin rectangular plates with arbitrary boundary conditions. *Int J Struct Stab Dyn* 2011;**11(1)**:1-21.
12. Yüzbaşı S, Sezer M. An Exponential matrix method for solving systems of linear differential equations. *Math Meth Appl Sciences* 2013;**36**(3):336-48.
13. Shamhorad S. Numerical solution of general form linear Fredhom Volterra integro differential equations by the Tau method with an error estimation. *Appl Math and Comput* 2005;**167**:141829.
14. Karampour H, Albermani F, Gross J. On lateral and upheaval buckling of subsea pipelines. *Eng Struct* 2013;**52:**317-30.